Inorganica Chimica Acta, 178 (1990) 261-267

Molecular structure of bis(1-methylimidazole)(*meso*-tetraphenylporphinato)iron(III) perchlorate

Thomas B. Higgins*, Martin K. Safo and **W. Robert Scheidt****
Department of Chemistry and Biochemistry, University of Notre Dame, Notre Dame, IN 46556 (U.S.A.)

(Received July 30, 1990)

Abstract

The preparation and characterization of the bis(1-methylimidazole)(*meso*-tetraphenylporphinato)iron(III) perchlorate complex is described. The molecular structure has been determined by an X-ray crystal structure determination. The complex has two axial imidazole ligands that are nearly coplanar and close to eclipsing an Fe–N_p bond. A rhombic distortion in the equatorial bonds is seen; the set that is approximately perpendicular to the imidazole ligand planes has an average value of 1.973(6) Å while the other set has an average value of 1.991(4) Å. The axial Fe–N(Im) bond distances average to 1.974 Å. The complex has a rhombic EPR spectrum and the derived crystal field parameters are reported. Crystal data: $a=10.730(1)$, $b=21.207(4)$, $c=21.231(4)$ Å, and $\beta=96.82(1)°$, monoclinic, space group $P2_1/n$, $V=4796.8$ Å^3, $Z=4$, $R_1=0.066$, $R_2=0.074$ based on 6429 observed data.

Introduction

In earlier work, we have shown that the orientation of planar axial ligands in iron(III) porphyrinate derivatives can have a profound effect on the electronic structure of the iron atom. The axial ligand orientation is given by the projection of the planar ligand onto the porphinato core, with the orientation angle defined by how close the projected plane falls to a Fe–N_p vector. This angle is frequently called ϕ and can take values between 0 and 45°. For imidazole ligands, the observed ϕ values [1] are typically rather small. Secondly, when there are two ligands, the dihedral angle between the two ligand planes defines the relative orientation; the limiting cases are parallel (coplanar) and perpendicular relative orientations.

We have found that the *relative* orientation of the axial is correlated with the nature of the EPR spectrum with parallel or approximately parallel orientations giving the well-known low-spin rhombic EPR spectrum. We [2] and others [3] have shown that the electron paramagnetic resonance (EPR) spectra of such bis-complexed low-spin derivatives also appears to be sensitive to absolute axial ligand orientation. We have also shown [2] that the perpendicular relative orientation leads to an unusual EPR spectrum which we call 'large g_{max}'†; this spectrum consists of a single observed line (at very low temperatures) with a relatively high g value ($g>3.3$). We have noted that the electronic structure that leads to such large g_{max} species might play a significant role [2] in modulating the reduction potentials of bis-histidine coordinated electron transfer heme proteins.

In this paper, we report the molecular structure and EPR spectrum of the bis(imidazole) complex, $[Fe(TPP)(1\text{-MeIm})_2]ClO_4$††. This complex represents the uncommon case in which the relative axial ligand

---

*Visiting student from Kalamazoo College.

**Author to whom correspondence should be addressed.

†This EPR spectral feature has also been termed 'HALS' (highly anisotropic low-spin) and 'strong g_{max}'. Both terminologies are somewhat misleading as greater anisotropy in the g-tensor normally leads to a smaller calculated rhombicity V/Δ (complex is less rhombic, more tetragonal); moreover, the observed intensity of this spectral feature is very temperature dependent and in general the amplitude, in derivative mode of the one observed feature, is no greater than that of any one rhombic EPR signal at the same temperature.

††Abbreviations used: TPP and TMP, dianions of *meso*-tetraphenylporphyrin and *meso*-tetramesitylporphyrin; Proto IX, dianion of protoporphyrin IX; Py, pyridine; 3-ClPy, 3-chloropyridine; HIm, imidazole; 1-MeIm, 1-methylimidazole; 2-MeHIm, 2-methylimidazole; c-MU and t-MU, *cis*- and *trans*-methyl urocanate (methyl 4-imidazoleacrylate); THF, tetrahydrofuran; N_p porphinato nitrogen; N_{ax}, axial nitrogen.

0020-1693/90/$3.50

orientation is approximately parallel rather than precisely parallel with required inversion symmetry as found in refs. 4–6 in almost all previously characterized bis(imidazole) iron(III) porphyrinate complexes.

Experimental

Solvents (CH_2Cl_2, THF and hexane) were distilled under argon prior to use. [Fe(TPP)($OClO_3$)] was prepared by the method of Dolphin *et al.* [7]; 3-chloropyridine and 1-methylimidazole were obtained from Aldrich and were used without further purification. A 1:4:1 molar ratio of [Fe(TPP)($OClO_3$)] (50 mg, 0.062 mmol), 3-chloropyridine (0.248 mmol), and 1-methylimidazole (0.062 mmol) were dissolved in 4 ml CH_2Cl_2. The solution was transferred to a 16×150 mm test tube and layered with hexane. The layered tube was allowed to stand for 72 h, during which time suitable X-ray quality crystals formed. An EPR powder spectrum was obtained on a Varian E-Line spectrometer at 77 K; selected single crystals from the above preparation were crushed and used for this solid-state measurement. A solution EPR spectrum of [Fe(TPP)(1-MeIm)$_2$]ClO_4 was obtained by adding an excess of 1-methylimidazole to a CH_2Cl_2 solution of [Fe(TPP)($OClO_3$)].

Structure determination

Preliminary examination of a crystal on a Syntex P$\bar{1}$ diffractometer with Mo Kα radiation led to the assignment of a four-molecule, primitive monoclinic unit cell. Subsequent data collection on an Enraf-Nonius CAD4 diffractometer with graphite-monochromated Mo Kα radiation led to the unique assignment of space group $P2_1/n$. Least-squares refinement of 25 automatically centered reflections gave the cell constants reported in Table 1. Intensity data for the complex were measured as described in Table 1. Intensity data were reduced using the BEGIN program in SDP [8]. The structure was solved using direct methods programs and difference Fourier techniques. (Programs used in this study were local modifications of those given in ref. 9a). Atomic form factors were from ref. 9b; real and imaginary corrections for anomalous dispersion in the form factor of the iron and chlorine atoms were from ref. 9c; scattering factors for hydrogen were from ref. 9d; all calculations were performed on a VAX 3200 computer. After several cycles of full-matrix least-squares refinements, it was clear that the molecule was the bis(1-methylimidazole) complex and the perchlorate anion and methylene chloride solvent molecule were disordered. The disordered CH_2Cl_2 solvate was modeled using four chlorine atom positions, while the perchlorate anion was described by using eight oxygen atom positions and a single central chlorine position. Further difference Fourier syntheses suggested the positions of the hydrogen atoms of the molecule, which were added in idealized positions as fixed contributors (C–H = 0.95 Å, **B**(H) = 1.3 × **B**(C)). The least-squares refinement was carried to convergence with anisotropic thermal parameters for all atoms save two of the disordered oxygen atoms of the perchlorate. Fractional atomic coordinates are listed in Table 2. See also 'Supplementary material'.

TABLE 1. Crystal data and intensity collection parameters

Complex	[Fe(TPP)(1-MeIm)$_2$]$ClO_4 \cdot CH_2Cl_2$
Formula	$FeCl_3O_4N_8C_{53}H_{42}$
Formula weight (amu)	1017.2
Space group	$P2_1/n$
T (K)	298
a (Å)	10.730(1)
b (Å)	21.207(4)
c (Å)	21.231(4)
β (°)	96.82(1)
V (Å^3)	4796.8
Z	4
Scan technique	θ–2θ
Diffractometer	CAD4
Crystal dimensions (mm)	0.40×0.50×0.70
2θ limits	4.0–52.8
Radiation	Mo Kα
Criterion for observation	$F_o > 3.0\sigma(F_o)$
No. observed data	6429
D_{obs} (g/cm^3)	1.37
D_{calc} g/cm^3)	1.37
R_1	0.066
R_2	0.074

Results

The solid-state structure of [Fe(TPP)(1-MeIm)$_2$]ClO_4 consists of a full independent molecule in an asymmetric unit of structure with no required symmetry. An ORTEP diagram of the complex is shown in Fig. 1, along with the atom numbering scheme. The bond distances in the coordination group are also shown. A complete listing of bond distances and bond angles is given in Tables 3 and 4.

The axial ligands of the [Fe(TPP)(1-MeIm)$_2$]ClO_4 complex form ϕ angles of 22 and 32° with an angle of 10° separating the ligand planes. The complex also shows an uncommon S_4-ruffling of the porphyrin core. A view of the ligand orientations relative to

TABLE 2. Fractional coordinates for $[Fe(TPP)(1\text{-}MeIm)_2]ClO_4 \cdot CH_2Cl_2$[a]

Atom	x	y	z
Fe	0.42564(5)	0.087879(25)	0.199671(25)
N(1)	0.58588(27)	0.08506(14)	0.25542(14)
N(2)	0.48561(27)	0.16404(14)	0.15772(14)
N(3)	0.26618(27)	0.09023(15)	0.14257(14)
N(4)	0.36363(27)	0.01352(14)	0.24419(15)
N(5)	0.35394(27)	0.14300(15)	0.26136(14)
N(6)	0.49707(27)	0.03113(14)	0.13986(14)
N(7)	0.22946(28)	0.17516(17)	0.33015(15)
N(8)	0.6127(3)	−0.00503(16)	0.06962(15)
C(a1)	0.6190(3)	0.04368(18)	0.30450(18)
C(a2)	0.6922(3)	0.12161(19)	0.25191(17)
C(a3)	0.5982(3)	0.19465(18)	0.17199(18)
C(a4)	0.4175(4)	0.19968(19)	0.11177(18)
C(a5)	0.2331(3)	0.13160(19)	0.09284(18)
C(a6)	0.1675(3)	0.04780(19)	0.13992(18)
C(a7)	0.2495(3)	−0.01624(18)	0.23122(19)
C(a8)	0.4221(4)	−0.01519(19)	0.29791(19)
C(b1)	0.7475(4)	0.05317(21)	0.33006(19)
C(b2)	0.7911(4)	0.10072(20)	0.29707(20)
C(b3)	0.5976(4)	0.25246(20)	0.13643(21)
C(b4)	0.4864(4)	0.25526(20)	0.09995(21)
C(b5)	0.1159(4)	0.11385(21)	0.05882(19)
C(b6)	0.0761(4)	0.06251(21)	0.08783(19)
C(b7)	0.2368(4)	−0.06388(21)	0.27744(21)
C(b8)	0.3414(4)	−0.06302(21)	0.31894(21)
C(m1)	0.6984(3)	0.17368(19)	0.21304(18)
C(m2)	0.3024(3)	0.18402(19)	0.07880(18)
C(m3)	0.1584(3)	−0.00137(19)	0.18236(19)
C(m4)	0.5421(4)	−0.00198(19)	0.32704(19)
C(11)	0.8193(3)	0.20958(19)	0.21832(18)
C(12)	0.9179(4)	0.18932(23)	0.18731(21)
C(13)	1.0301(4)	0.22262(28)	0.19415(24)
C(14)	1.0439(4)	0.27528(27)	0.23008(26)
C(15)	0.9461(5)	0.29634(24)	0.26107(24)
C(16)	0.8341(4)	0.26340(22)	0.25467(21)
C(21)	0.2538(4)	0.22473(19)	0.02404(19)
C(22)	0.3224(4)	0.23133(21)	−0.02703(21)
C(23)	0.2799(5)	0.26978(25)	−0.07744(22)
C(24)	0.1688(5)	0.30150(26)	−0.07845(25)
C(25)	0.0997(5)	0.29462(27)	−0.02898(28)
C(26)	0.1408(4)	0.25663(24)	0.02228(22)
C(31)	0.0400(4)	−0.03986(20)	0.17480(19)
C(32)	−0.0643(4)	−0.02018(24)	0.20152(22)
C(33)	−0.1730(4)	−0.0560(3)	0.19437(25)
C(34)	−0.1787(5)	−0.11046(27)	0.16074(26)
C(35)	−0.0762(5)	−0.12996(24)	0.13296(26)
C(36)	0.0339(4)	−0.09496(23)	0.14011(24)
C(41)	0.5903(4)	−0.03791(21)	0.38513(20)
C(42)	0.6120(4)	−0.10230(24)	0.38235(24)
C(43)	0.6534(5)	−0.1355(3)	0.4361(3)
C(44)	0.6745(6)	−0.1050(4)	0.4932(3)
C(45)	0.6576(5)	−0.0417(4)	0.49698(25)
C(46)	0.6143(5)	−0.00717(25)	0.44242(23)
C(1)	0.2528(4)	0.13055(20)	0.28941(19)
C(2)	0.3964(4)	0.19949(23)	0.28580(23)
C(3)	0.3217(5)	0.22005(24)	0.32850(24)
C(4)	0.1188(4)	0.17498(29)	0.36619(21)
C(5)	0.5891(4)	0.04455(19)	0.10542(19)
C(6)	0.4625(4)	−0.02992(20)	0.12558(21)
C(7)	0.5332(4)	−0.05233(21)	0.08232(22)
C(8)	0.7109(4)	−0.00927(24)	0.02713(22)
Cl(1)	−0.26689(14)	0.17752(7)	−0.01824(7)
O(1)	−0.1786(15)	0.2214(7)	−0.0166(8)
O(2)	−0.3728(7)	0.1556(4)	0.0115(4)
O(3)	−0.2610(26)	0.1500(12)	−0.0692(11)
O(4)	−0.1667(9)	0.1379(8)	−0.0048(8)
O(5)	−0.3158(13)	0.1659(6)	−0.0850(6)
O(6)	−0.2399(20)	0.1476(6)	0.0404(5)
O(7)	−0.3774(25)	0.1903(14)	−0.0191(13)
O(8)	−0.2726(13)	0.2441(4)	−0.0103(5)
C(S)	0.0387(8)	0.0745(5)	−0.4443(6)
Cl(2)	−0.1112(17)	0.0884(6)	−0.4781(8)
Cl(3)	−0.0541(5)	0.0117(4)	−0.39100(27)
Cl(4)	0.0016(11)	0.0669(4)	−0.3800(4)
Cl(5)	−0.0710(7)	0.09948(25)	−0.50420(28)

[a] e.s.d.s of the least significant digits are given in parentheses.

each other and to the porphyrin core is shown in Fig. 2, along with the deviations of each atom from the best porphyrin plane (in units of 0.01 Å). Averaged values of bond distances and angles in the porphyrin core are also shown.

The EPR spectra of $[Fe(TPP)(1\text{-}MeIm)_2]ClO_4$, taken either as a powder (crushed single crystals) or as a frozen solution, are rhombic and typical of low-spin iron(III) hemes. The frozen solution spectrum has $g_z = 2.890$, $g_y = 2.291$ and $g_x = 1.554$. Unfortunately, the powder spectrum is not particularly well resolved; our best estimates for the principal g values are $g_z = 2.866$, $g_y = 2.297$ and $g_x = 1.577$*.

Discussion

The structure of the $[Fe(TPP)(1\text{-}MeIm)_2]ClO_4$ complex shows a number of interesting features that merit individual discussion. A comparison of the structural parameters of this complex with all previously reported low-spin bis(imidazole) and -(pyridine) complexes is given in Table 5. The average axial Fe–N(Im) distance of 1.974(6) Å is typical of distances observed previously with unhindered imidazole derivatives. The equatorial Fe–N_p distances differ in a way that correlates with the absolute orientation of the axial ligands. As can be seen from an examination of Fig. 2, the equatorial Fe–N_p bonds that are approximately perpendicular to the imidazole ring planes are significantly shorter than the set that are approximately parallel to the imidazole planes;

---

*Both spectra satisfy the Griffith relationship $g_z^2 + g_y^2 + g_x^2 = 16$ to within ±0.02.

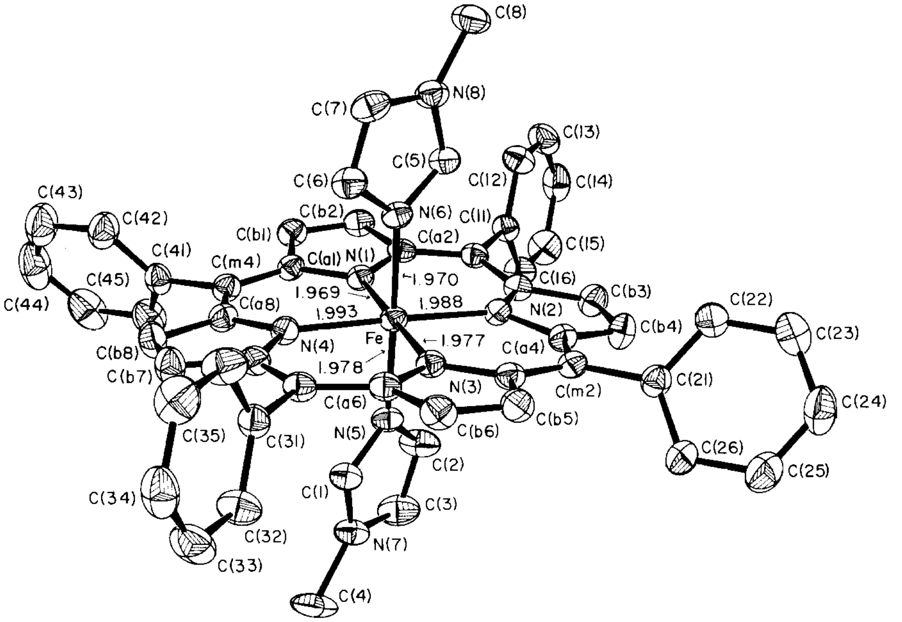

Fig. 1. ORTEP diagram of $[Fe(TPP)(1\text{-}MeIm)_2]ClO_4$ showing the atom labels assigned to each atom. Atoms are contoured at the 30% probability level.

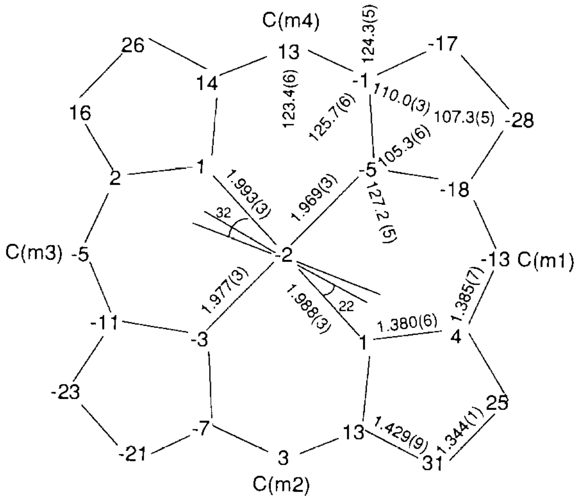

Fig. 2. Formal diagram of the porphinato core in $[Fe(TPP)(1\text{-}MeIm)_2]ClO_4$ showing the relative orientations of the axial ligands with each other and the $Fe\text{-}N_p$ vectors. Also displayed in this diagram are the displacements of each atom, in units of 0.01 Å, from the best plane of the 24-atom porphinato core. Averaged values of bond distances and angles in the core are given.

the respective averaged values are 1.973 and 1.991 Å. The appearance of such a rhombic distortion in the equatorial distances was first noted for $[Fe(TPP)(HIm)_2]\cdot CHCl_3$ [5]. As we have noted earlier [5], we believe that this structural rhombicity results from π bonding effects. The π-donating ability of imidazole requires that the half-filled iron orbital, conventionally taken as d_{yz}, be aligned effectively perpendicular to the imidazole plane. Of course, the other filled π orbital (d_{xz}) is then parallel to the imidazole plane. When the imidazole planes lie near $Fe\text{-}N_p$ vectors, then the dπ orbitals must be oriented so the porphyrin ligand is able to π-donate only to the half-filled d_{yz} orbital and not to the filled d_{xz} orbital. We thus expect shorter $Fe\text{-}N_p$ distances in the direction perpendicular to the imidazole planes. The $Fe\text{-}N_p$ distances marked with an asterisk in Table 5 show the expected rhombic distortion as a result of an imidazole ligand orientation nearly along the $Fe\text{-}N_p$ bonds.

The porphinato core in $[Fe(TPP)(1\text{-}MeIm)_2]ClO_4$ is decidedly non-planar as can be seen from an inspection of Fig. 2. The pattern of atom displacements in the porphinato core correspond closely to those required by exact D_{2d} symmetry, often simply called S_4-ruffling. However, the ruffling pattern has a somewhat unexpected feature. Porphinato cores can have two different idealized forms of $S_4(D_{2d})$-ruffling. These differ by a rotation of the symmetry elements by 45° about the axis normal to the plane. Thus, the methine carbons (C_m) are either alternately above and below the porphyrin plane or are on the mean porphyrin plane. The former conformation is more common; the latter has the saddle-shaped surface described for the π-cation species with both β-carbon atoms of the pyrrole rings alternatively above or below the mean plane of the 24-atom core. Scheidt and Lee [14] have tabulated core confor-

TABLE 3. Bond distances in [Fe(TPP)(1-MeIm)$_2$]ClO$_4$·CH$_2$Cl$_2$

Type	Value (Å)	Type	Value (Å)
Fe–N(1)	1.969(3)	C(12)–C(13)	1.388(6)
Fe–N(2)	1.988(3)	C(13)–C(14)	1.351(7)
Fe–N(3)	1.977(3)	C(14)–C(15)	1.378(7)
Fe–N(4)	1.993(3)	C(15)–C(16)	1.383(6)
Fe–N(5)	1.978(3)	C(16)–C(11)	1.376(6)
Fe–N(6)	1.970(3)	C(21)–C(22)	1.388(5)
N(1)–C(a1)	1.376(5)	C(22)–C(23)	1.379(6)
N(1)–C(a2)	1.389(4)	C(23)–C(24)	1.367(7)
N(2)–C(a3)	1.374(4)	C(24)–C(25)	1.363(7)
N(2)–C(a4)	1.374(5)	C(25)–C(26)	1.384(6)
N(3)–C(a5)	1.386(5)	C(26)–C(21)	1.385(5)
N(3)–C(a6)	1.385(5)	C(31)–C(32)	1.378(6)
N(4)–C(a7)	1.376(4)	C(32)–C(33)	1.385(6)
N(4)–C(a8)	1.377(5)	C(33)–C(34)	1.356(7)
N(5)–C(1)	1.324(3)	C(34)–C(35)	1.372(7)
N(5)–C(2)	1.363(3)	C(35)–C(36)	1.388(6)
N(6)–C(5)	1.328(3)	C(36)–C(31)	1.379(6)
N(6)–C(6)	1.371(3)	C(41)–C(42)	1.388(6)
C(a1)–C(b1)	1.435(5)	C(42)–C(43)	1.370(7)
C(a1)–C(m4)	1.393(5)	C(43)–C(44)	1.368(9)
C(a2)–C(b2)	1.414(5)	C(44)–C(45)	1.358(9)
C(a2)–C(m1)	1.385(5)	C(45)–C(46)	1.402(7)
C(a3)–C(b3)	1.439(5)	C(46)–C(41)	1.377(6)
C(a3)–C(m1)	1.375(5)	C(1)–N(7)	1.326(5)
C(a4)–C(b4)	1.429(6)	N(7)–C(3)	1.377(6)
C(a4)–C(m2)	1.386(5)	N(7)–C(4)	1.487(5)
C(a5)–C(b5)	1.425(5)	C(3)–C(2)	1.352(6)
C(a5)–C(m2)	1.389(5)	C(5)–N(8)	1.339(5)
C(a6)–C(b6)	1.423(5)	N(8)–C(7)	1.365(5)
C(a6)–C(m3)	1.389(5)	N(8)–C(8)	1.469(5)
C(a7)–C(b7)	1.426(5)	C(7)–C(6)	1.346(6)
C(a7)–C(m3)	1.375(5)	Cl(1)–O(1)	1.326(11)
C(a8)–C(b8)	1.438(5)	Cl(1)–O(2)	1.441(7)
C(a8)–C(m4)	1.389(5)	Cl(1)–O(3)	1.238(15)
C(b1)–C(b2)	1.343(5)	Cl(1)–O(4)	1.367(10)
C(b3)–C(b4)	1.345(6)	Cl(1)–O(5)	1.473(11)
C(b5)–C(b6)	1.345(6)	Cl(1)–O(6)	1.392(10)
C(b7)–C(b8)	1.342(6)	Cl(1)–O(7)	1.215(26)
C(m1)–C(11)	1.497(4)	Cl(1)–O(8)	1.425(9)
C(m2)–C(21)	1.492(4)	C(s)–Cl(2)	1.707(17)
C(m3)–C(31)	1.503(4)	C(s)–Cl(3)	2.077(13)
C(m4)–C(41)	1.489(4)	C(s)–Cl(4)	1.476(12)
C(11)–C(12)	1.379(5)	C(s)–Cl(5)	1.710(13)

TABLE 4. Bond angles in [Fe(TPP)(1-MeIm)$_2$]ClO$_4$·CH$_2$Cl$_2$

Type	Value (°)	Type	Value (°)
N(1)–Fe–N(2)	89.3(1)	C(a4)–C(m2)–C(21)	117.6(3)
N(1)–Fe–N(3)	179.1(1)	C(a5)–C(m2)–C(21)	119.0(3)
N(1)–Fe–N(4)	90.4(1)	C(a6)–C(m3)–C(a7)	124.3(4)
N(1)–Fe–N(5)	90.0(1)	C(a6)–C(m3)–C(31)	117.5(3)
N(1)–Fe–N(6)	89.4(1)	C(a7)–C(m3)–C(31)	118.2(3)
N(2)–Fe–N(3)	90.4(1)	C(a8)–C(m4)–C(a1)	122.9(4)
N(2)–Fe–N(4)	177.9(1)	C(a8)–C(m4)–C(41)	118.6(3)
N(2)–Fe–N(5)	89.3(1)	C(a1)–C(m4)–C(41)	118.6(3)
N(2)–Fe–N(6)	92.1(1)	C(m1)–C(11)–C(12)	120.8(4)
N(3)–Fe–N(4)	89.9(1)	C(m1)–C(11)–C(16)	120.3(4)
N(3)–Fe–N(5)	90.8(1)	C(12)–C(11)–C(16)	118.9(4)
N(3)–Fe–N(6)	89.7(1)	C(11)–C(12)–C(13)	119.7(4)
N(4)–Fe–N(5)	88.6(1)	C(12)–C(13)–C(14)	121.0(5)
N(4)–Fe–N(6)	90.0(1)	C(13)–C(14)–C(15)	119.9(4)
N(5)–Fe–N(6)	178.5(1)	C(14)–C(15)–C(16)	119.5(5)
Fe–N(1)–C(a1)	127.1(3)	C(11)–C(16)–C(15)	121.0(4)
Fe–N(1)–C(a2)	128.0(3)	C(m2)–C(21)–C(22)	119.9(4)
C(a1)–N(1)–C(a2)	104.9(3)	C(m2)–C(21)–C(26)	121.8(4)
Fe–N(2)–C(a3)	127.5(3)	C(22)–C(21)–C(26)	118.2(4)
Fe–N(2)–C(a4)	126.3(2)	C(21)–C(22)–C(23)	120.6(4)
C(a3)–N(2)–C(a4)	106.1(3)	C(22)–C(23)–C(24)	120.7(4)
Fe–N(3)–C(a5)	127.4(2)	C(23)–C(24)–C(25)	119.2(5)
Fe–N(3)–C(a6)	127.6(3)	C(24)–C(25)–C(26)	121.1(5)
C(a5)–N(3)–C(a6)	104.8(3)	C(21)–C(26)–C(25)	120.1(4)
Fe–N(4)–C(a7)	127.4(3)	C(m3)–C(31)–C(32)	120.6(4)
Fe–N(4)–C(a8)	126.7(3)	C(m3)–C(31)–C(36)	120.2(4)
C(a7)–N(4)–C(a8)	105.7(3)	C(32)–C(31)–C(36)	119.2(4)
Fe–N(5)–C(1)	125.7(2)	C(31)–C(32)–C(33)	120.2(5)
Fe–N(5)–C(2)	129.3(2)	C(32)–C(33)–C(34)	120.6(5)
C(1)–N(5)–C(2)	105.0(2)	C(33)–C(34)–C(35)	119.7(5)
Fe–N(6)–C(5)	126.6(2)	C(34)–C(35)–C(36)	120.5(5)
Fe–N(6)–C(6)	127.1(2)	C(31)–C(36)–C(35)	119.8(4)
C(5)–N(6)–C(6)	106.3(3)	C(m4)–C(41)–C(42)	120.8(4)
N(1)–C(a1)–C(b1)	110.3(3)	C(m4)–C(41)–C(46)	120.0(4)
C(b1)–C(a1)–C(m4)	123.3(4)	C(42)–C(41)–C(46)	119.3(4)
N(1)–C(a1)–C(m4)	126.4(3)	C(41)–C(42)–C(43)	120.7(5)
N(1)–C(a2)–C(b2)	110.1(3)	C(42)–C(43)–C(44)	119.8(6)
C(b2)–C(a2)–C(m1)	124.6(4)	C(43)–C(44)–C(45)	120.8(6)
N(1)–C(a2)–C(m1)	125.1(3)	C(44)–C(45)–C(46)	120.0(6)
N(2)–C(a3)–C(b3)	109.8(3)	C(41)–C(46)–C(45)	119.4(5)
C(b3)–C(a3)–C(m1)	124.2(4)	N(5)–C(1)–N(7)	112.3(4)
N(2)–C(a3)–C(m1)	126.0(4)	C(1)–N(7)–C(3)	106.5(3)
N(2)–C(a4)–C(b4)	109.6(3)	C(1)–N(7)–C(4)	123.9(4)
C(b4)–C(a4)–C(m2)	123.9(4)	C(3)–N(7)–C(4)	129.5(4)
N(2)–C(a4)–C(m2)	126.4(4)	N(7)–C(3)–C(2)	106.2(4)
N(3)–C(a5)–C(b5)	110.5(3)	C(3)–C(2)–N(5)	109.9(4)
C(b5)–C(a5)–C(m2)	124.4(4)	N(6)–C(5)–N(8)	110.3(4)
N(3)–C(a5)–C(m2)	125.1(3)	C(5)–N(8)–C(7)	107.5(3)
N(3)–C(a6)–C(b6)	110.0(3)	C(5)–N(8)–C(8)	126.5(4)
C(b6)–C(a6)–C(m3)	125.0(4)	C(7)–N(8)–C(8)	126.0(4)
N(3)–C(a6)–C(m3)	125.0(3)	N(8)–C(7)–C(6)	107.0(4)
N(4)–C(a7)–C(b7)	110.0(3)	C(7)–C(6)–N(6)	108.9(4)
C(b7)–C(a7)–C(m3)	124.4(4)	O(1)–Cl(1)–O(2)	144.4(10)
N(4)–C(a7)–C(m3)	125.6(4)	O(1)–Cl(1)–O(3)	104.1(13)
N(4)–C(a8)–C(b8)	109.7(3)	O(1)–Cl(1)–O(4)	83.3(9)
C(b8)–C(a8)–C(m4)	124.3(4)	O(2)–Cl(1)–O(3)	110.9(10)
N(4)–C(a8)–C(m4)	125.9(4)	O(2)–Cl(1)–O(4)	110.6(7)
C(a1)–C(b1)–C(b2)	106.7(3)	O(3)–Cl(1)–O(4)	76.8(14)
C(a2)–C(b2)–C(b1)	108.0(3)	O(2)–Cl(1)–O(6)	142.6(7)
C(a3)–C(b3)–C(b4)	106.7(4)	O(5)–Cl(1)–O(7)	77.8(14)
C(a4)–C(b4)–C(b3)	107.7(4)	O(5)–Cl(1)–O(8)	105.3(7)

(continued)

mations for all tetraphenylporphyrin complexes; the core conformation pattern of [Fe(TPP)(1-MeIm)$_2$]ClO$_4$ is not commonly seen in six-coordinate derivatives. Such ruffling patterns appear to result from non-bonded interactions between peripheral phenyl rings, at least one of which has a dihedral angle with the porphyrin core less than ~60°. The fact that two of the observed dihedral angles are small is consistent with the core conformation (the four values are 86.1, 56.1, 82.8, and 61.9°). Also given in Table 5 is information on porphinato core conformations in these iron(III) derivatives. Average

TABLE 4 (*continued*)

Type	Value (°)	Type	Value (°)
C(a5)–C(b5)–C(b6)	106.9(3)	O(6)–Cl(1)–O(7)	102.3(13)
C(a6)–C(b6)–C(b5)	107.8(4)	O(6)–Cl(1)–O(8)	110.6(8)
C(a7)–C(b7)–C(b8)	107.6(4)	O(7)–Cl(1)–O(8)	74.0(13)
C(a8)–C(b8)–C(b7)	107.0(4)	Cl(2)–C(s)–Cl(3)	81.4(7)
C(a2)–C(m1)–C(a3)	123.1(3)	Cl(2)–C(s)–Cl(4)	93.6(9)
C(a2)–C(m1)–C(11)	117.6(3)	Cl(2)–C(s)–Cl(5)	26.3(7)
C(a3)–C(m1)–C(11)	119.2(3)	Cl(3)–C(s)–Cl(4)	39.3(5)
C(a4)–C(m2)–C(a5)	123.4(4)	Cl(3)–C(s)–Cl(5)	105.8(5)
		Cl(4)–C(s)–Cl(5)	118.9(7)

absolute values of the displacements of the *meso*- and β-carbon atoms of the porphinato core are given along with the average value of displacement for all atoms of the core. Finally a summary of absolute and relative axial ligand orientations is given.

The electronic structure of [Fe(TPP)(1-MeIm)$_2$]ClO$_4$ is rhombic and is described in terms of crystal field parameters, Δ and V, as shown in Fig. 3. Values of Δ and V, in terms of the spin–orbit coupling constant λ, can be determined from the principal EPR g values using the expressions given by Taylor [15]. Using the solid state g values yields $\Delta/\lambda = 3.16$ and $V/\lambda = 2.01$. These values appear within the range of those observed by Walker *et al.* for the bis(1-methylimidazole) complexes of [Fe(TPP)(Cl)] and [Fe(TPP)(I)] [16] in chloroform solution. More interestingly, Strouse and coworkers [17, 18] have suggested that the rhombicity parameter V/Δ of Blumberg and Peisach [19] should be related to the ligand orientation angle ϕ. They presented such a correlation [18] for five bis(N–H imidazole) complexes with known orientation angles and obtained a reasonable relationship for V/Δ versus ϕ. Their correlation of rhombicity with geometry predicts a value of $V/\Delta = 0.58$–0.54 for ligand orientations ϕ between 22 and 32°, far smaller than the observed value of 0.635 for [Fe(TPP)(1-MeIm)$_2$]ClO$_4$. That value (0.635) is predicted for complexes with ϕ near 0°. There are two possible explanations for the relatively poor agreement with correlation of Strouse and coworkers. The poor agreement may result from using a correlation derived for N–H imidazole derivatives for an N–R imidazole complex. Significantly different pK_a versus ligand binding equilibrium constant relationships for N–H versus N–R imidazoles have been described [20]. Secondly, the correlation was derived from a series of complexes having precisely parallel ligand planes rather than the approximately parallel set in [Fe(TPP)(1-MeIm)$_2$]ClO$_4$; the 10° difference in ligand planes could have a significant effect on the crystal field values. There remains the possibility that a correlation of rhombicity

TABLE 5. Summary of Fe–N bond distances, core conformation and ligand orientation in low-spin six-coordinate pyridine and imidazole derivatives

Complex	Fe–N$_p$^{a}	Fe–N$_{ax}$$^{a, b}$	C$_m$$^{c, d}$	C$_b$$^{c, d}$	C$_{av}$$^{c, d}$	C$_{max}$$^{d, e}$	ϕ^{f}	$\Delta\phi$^{f}	Reference
[Fe(TPP)(2-MeHIm)$_2$]ClO$_4$	1.971(4)	2.015(4) 2.010(4)	40	17	21	41	32 32	89	13
[Fe(TPP)(HIm)$_2$]Cl·MeOH	1.989(8)	1.991(5) 1.957(4)	31	12	16	33	18 39	57	10
[Fe(TPP)(Py)$_2$]ClO$_4$	1.982(7)	2.005(5) 2.001(5)	25	14	14	29	34 38	86	3
[Fe(TPP)(1-MeIm)$_2$]ClO$_4$	1.982(11)*	1.970(3) 1.978(3)	9	23	12	31	22 32	11	this work
[Fe(ProtoIX)(1-MeIm)$_2$]	1.991(16)*	1.988(5) 1.966(5)	14	7	7	13	3 16	13	11
[Fe(TMP)(1-MeIm)$_2$]ClO$_4$	1.988(20)* 1.987(1)	1.975(3) 1.965(3)	1 8	2 7	1 5	4 9	23 41	0 0	6
[Fe(OEP)(3-ClPy)$_2$]ClO$_4$	1.995(6)	2.031(2)	3	4	3	6	41	0	12
[Fe(TPP)(HIm)$_2$]Cl·CHCl$_3$	1.994(12)* 1.993(4)	1.977(3) 1.964(3)	0 4	2 2	1 2	4 7	6 41	0 0	5
[Fe(TPP)(c-MU)$_2$]SbF$_6$	1.995(17)* 1.997(1)	1.979(7) 1.967(7)	4 2	2 1	3 1	6 2	16 29	0 0	4
[Fe(TPP)(t-MU)$_2$]SbF$_6$	1.992(5)	1.983(4)	1	2	2	4	22	0	4

[a] Values in Å. [b] N$_{ax}$ is the pyridine or imidazole ligand nitrogen atom. [c] Average absolute value of displacements of the methine carbons (C$_m$), beta carbons (C$_b$) and the 24-atom (C$_{av}$) from the 24-atom core plane. [d] Values in units of 0.01 Å. [e] Maximum absolute displacement of any core atom from the 24-atom core plane. [f] Values in units of degrees.

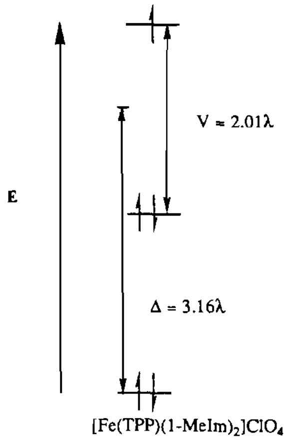

Fig. 3. Energy level diagram for low-spin bis(imidazole) iron(III) porphyrinate derivatives.

versus geometry cannot be accurately quantified for a wide variety of imidazole ligands in the solid state; further work will be required to evaluate this possibility.

Supplementary material

Table S1, anisotropic thermal parameters; Table S2, fixed hydrogen atom positions and a table of observed and calculated structure amplitudes (×10) are available from the authors on request.

Acknowledgement

We thank the U.S. National Institutes of Health (Grant GM-38401) for support of this research.

References

1 W. R. Scheidt and D. M. Chipman, *J. Am. Chem. Soc., 108* (1986) 1163.
2 F. A. Walker, B. H. Huynh, W. R. Scheidt and S. R. Osvath, *J. Am. chem. Soc., 108* (1986) 5288.
3 D. Inniss, M. Soltis and C. E. Strouse, *J. Am. Chem. Soc., 110* (1988) 5644.
4 R. Quinn, J. S. Valentine, M. P. Byrn and C. E. Strouse, *J. Am. Chem. Soc., 109* (1987) 3301.
5 W. R. Scheidt, S. R. Osvath and Y. J. Lee, *J. Am. Chem. Soc., 109* (1987) 1958.
6 M. K. Safo, G. P. Gupta, F. A. Walker and W. R. Scheidt, work in progress.
7 D. H. Dolphin, J. R. Sams and T. B. Tsin, *Inorg. Chem., 16* (1977) 711.
8 *SDP Instruction Manual*, Enraf-Nonius Corporation, 1986.
9 (a) P. Main, S. E. Hull, L. Lessinger, G. Germain, J.-P. Declercq and M. M. Woolfson, *MULTAN*, a system of computer programs for the automatic solution of crystal structures from X-ray diffraction data, Universities of York, U.K. and Louvain, Belgium, 1978; R. L. Lapp and R. A. Jacobson, *ALLS*, a generalized crystallographic least squares program, National Technical Information Services IS-4708 UC-4, Springfield, VI, U.S.A., 1979; W. R. Busing, K. O. Martin and H. A. Levy, *ORFFE, Rep. ORNL-TM-306*, Oak Ridge National Laboratory, TN, U.S.A., 1964; C. K. Johnson, *ORTEP2, Rep. ORNL-5138*, Oak Ridge National Laboratory, TN, U.S.A., 1976; *Zalkin's Fordap*; (b) D. T. Cromer and J. B. Mann, *Acta Crystallogr., Sect. A, 24* (1968) 321; (c) D. T. Cromer and D. J. Liberman, *J. Chem. Phys., 53* (1970) 1891; (d) R. F. Stewart, E. R. Davidson and W. T. Simpson, *J. Chem. Phys., 42* (1965) 3175.
10 R. Countryman, D. M. Collins and J. L. Hoard, *J. Am. Chem. Soc., 91* (1969) 5166.
11 R. G. Little, K. R. Dymock and J. A. Ibers, *J. Am. Chem. Soc., 97* (1975) 4532.
12 W. R. Scheidt, D. K. Geiger and K. J. Haller, *J. Am. Chem. Soc., 104* (1982) 495.
13 W. R. Scheidt, J. F. Kirner, J. L. Hoard and C. A. Reed, *J. Am. Chem. Soc., 109* (1987) 1963.
14 W. R. Scheidt and Y. J. Lee, *Struct. Bonding (Berlin), 64* (1987) 1.
15 C. P. S. Taylor, *Biochim. Biophys. Acta, 491* (1977) 137.
16 F. A. Walker, D. Reis and V. L. Balke, *J. Am. Chem. Soc., 106* (1984) 6888.
17 R. Quinn, J. S. Valentine, M. P. Byrn and C. E. Strouse, *J. Am. Chem. Soc., 109* (1987) 3301.
18 S. M. Soltis and C. E. Strouse, *J. Am. Chem. Soc., 110* (1988) 2824.
19 W. E. Blumberg and J. Peisach, *Adv. Chem. Ser., 100* (1971) 271.
20 F. A. Walker, M. W. Lo and M. T. Ree, *J. Am. Chem. Soc., 98* (1976) 5552.